X-625-71-73
PREPRINT

STUDIES OF POSITIVE ION COMPOSITION IN THE EQUATORIAL D-REGION IONOSPHERE

R. A. GOLDBERG
A. C. AIKIN

JULY 1971

GSFC

GODDARD SPACE FLIGHT CENTER
GREENBELT, MARYLAND

STUDIES OF POSITIVE ION COMPOSITION IN THE EQUATORIAL D REGION IONOSPHERE

by

R.A. Goldberg and A.C. Aikin
Laboratory for Planetary Atmospheres
NASA/Goddard Space Flight Center
Greenbelt, Maryland

ABSTRACT

Two daytime D region positive ion composition measurements at Thumba, India are presented for solar zenith angles of 53.2 and 27.8°. Comparison of upleg ram with downleg wake data shows a large increase in the concentration of heavy ions 48^+, $NO^+ \cdot H_2O$; 55^+, $H_3O^+ \cdot (H_2O)_2$; and $M^+ > 65^+$ for the downleg reduced shock condition. Peak concentrations of 48^+ and 55^+ occur at unit optical depth for Lyman alpha radiation. The ion 37^+, $H_3O^+ \cdot H_2O$, is dominant for $\chi = 27.8^\circ$ but not for $\chi = 53.2^\circ$, consistent above 80 km with an origin from the X-ray production of O_2^+. It is shown that NO^+ ions can be transferred to heavy hydrates 48^+, 55^+ and $M^+ > 65^+$ by a reaction chain starting with

$$NO^+ + X + M = NO^+ \cdot X + M$$

where X can be O_2, N_2, CO_2, or a combination of all three depending on the rate of reaction. This chain, together with a similar reaction scheme starting with O_2^+ and ending in 19^+, 37^+ and heavier clusters leads to a consistent explanation for the hydrated ions observed in the D region.

INTRODUCTION

Studies of the positive ion composition below 85 km have been conducted via sounding rockets employing quadrupole ion mass spectrometers housed in cryogenically cooled pumping systems for several years (e.g., Narcisi and Bailey, 1965; Narcisi, 1966, 1967, 1969; Narcisi and Roth, 1970). The results have shown that the D region below 85 km is dominated by hydrated water cluster ions having mass to charge ratios of 37^+, $H_3O^+ \cdot H_2O$; 55^+, $H_3O^+ \cdot (H_2O)_2$; 19^+, H_3O^+; and 48^+, $NO^+ \cdot H_2O$, instead of NO^+ as predicted.

The principal ionization source forming the undisturbed D region is the photoionization of nitric oxide (NO) by solar Lyman alpha radiation to produce NO^+. This is supplemented by solar X-rays at 2-8 Å and galactic cosmic radiation which produce O_2^+ and N_2^+ (Nicolet and Aikin, 1960). It is necessary to find a mechanism which will convert ions such as NO^+ and O_2^+ into hydrated cluster ions. Several mechanisms have been proposed, e.g. photoionization of CH_3 and its subsequent reaction with water (Swider, 1970), or the formation and ionization of submicronic ice nuclei (Hunt, 1969). Laboratory measurements have shown that a reaction scheme exists for the formation of the major ion 37^+ from O_2^+; this scheme has been applied to explain the origin of 37^+ in the D region (Ferguson and Fehsenfeld, 1969). Difficulties arise because it is assumed that large concentrations of O_2^+ are produced by the photoionization of $O_2(^1\Delta_g)$ as proposed by Hunten and McElroy (1968).

Neglect of CO_2 absorption of the ionizing radiation has led to a considerable overestimation of the importance of this source of ionization in the D region. Huffman et al., (1971). Application of the O_2^+ reaction scheme to NO^+ leads to the production of heavier clusters (e.g. 48^+, 55^+ and above) rather than 37^+, in disagreement with earlier measurements. Furthermore, it has been difficult to find the necessary reaction to start such a chain (Fehsenfeld and Ferguson, 1969). No satisfactory explanation has been proposed for the apparent absence of NO^+ coupled with currently accepted values for NO and the presence of heavier water clusters.

In this work we describe positive ion composition results obtained from measurements made at Thumba, India on March 19, 1970 for solar zenith angles of 53.2 and 27.8^{o}. The composition was measured using quadrupole ion mass spectrometers housed in titanium getter pumped systems similar to that described in Goldberg and Blumle (1970). Separation of the payload from the rocket motors permitted measurements to be carried out during both upleg ram and downleg wake sampling conditions for each flight. Also included in the payloads were experiments to measure positive ion and electron concentrations, Lyman alpha radiations, and the 2-8 $\mathring{A}$ solar X-ray spectrum. The results of these experiments are employed herein but are reported in detail elsewhere (Aikin et al., 1971; to be

referred to as Paper 1 throughout the remainder of this text).

Evidence is presented for the breakdown of ambient heavy cluster ions to 37^+ and possibly 19^+ by shock wave effects induced by the rocket motion. A qualitative comparison is made between the observed positive ion composition measured under weak shock (downleg wake) conditions and a theoretical model calculated from reactions involving the transformation of NO^+ and O_2^+ into cluster ions. These comparisons indicate the difficulties involved in presenting a quantative account of the positive ion distribution at D region altitudes.

EXPERIMENTAL DESCRIPTION

A. Rocket Description and Performance

The rockets, NASA 14.425 and NASA 14.424 were Nike Apaches supporting nine inch diameter bulbous payloads. In addition to an ion mass spectrometer, each payload included instruments to monitor solar Lyman alpha radiation, solar X-rays between 2-8 Å (14.425 only), and electron and ion density as described in Paper 1. Two axis magnetometers and solar aspect sensors were carried for attitude determination. The additional drag induced by the bulbous payload is responsible for the low apogees obtained. Figure 1 illustrates the performance of each payload in terms of Mach number. Figure 2 illustrates the front end configuration of the payload experiments.

Table 1 provides pertinent characteristics of flight performance and launch.

After second stage burnout, nose cone separation occurred followed by payload separation from the rocket motor and spectrometer cap ejection. Payload separation has two functions. First, it permits less probability of contamination from residual outgassing of the second rocket stage. Second, it reduces drag effects on the experimental system and causes the payload to remain in a fixed attitude position (if coning is neglected) to altitudes below 65 km on downleg. This feature enables direct upleg ram sampling to be compared with direct downleg wake sampling in the region of interest.

B. Spectrometer Characteristics

Both payloads contained quadrupole ion mass spectrometers housed in titanium getter pumped systems assisted by triode ion pumps as described in Goldberg and Blumle (1970). Modifications of that system include two ion pumps instead of one to double the efficiency of inert gas pumping; an off-center quadrupole rod assembly as illustrated in Figure 2 to permit space for additional complementary experiments; the increase of rod length from three to four inches for improved mass resolution; reduction in aperture size to allow less flow and longer pumping lifetimes. The spectrometer characteristics are shown in Table 2.

DATA REDUCTION OF ION COMPOSITION

Typical raw spectra from 14.424 are illustrated in Figure 3. These data are presented with the currents displayed on a logarithmic scale (ordinate) in which each volt is representative of approximately a full decade of sensitivity. Although not shown, the currents from 14.425 are found to be somewhat lower than those of 14.424, an effect due in part to the difference in solar zenith angle conditions but mainly caused by a variation in the mass resolution settings of the two instruments and the downleg operation of the 14.425 spectrometer at higher internal pressure. The degree of resolution is inversely related to sensitivity, and accuracy in setting two rocket instruments at the same resolution and maintaining such fixed values throughout a flight is affected by temperature changes and other paramters which may vary between flights. The higher pressure operating conditions for the spectrometer on 14.425 were induced by cap ejection at lower altitude. The differences in sensitivity between the two instruments are accounted for by the normalization processes.

The two horizontal ledges on the right hand side of each spectrum are results obtained in the high pass filter mode of the instrument, i.e. when the D.C. component of the field is set to zero. Two values are obtained in this mode. the first (A) containing all ions from $1 < M < \infty$, the

second (B) from 46, $49 \leq M < \infty$, for 14.424 or 14.425 respectively. Since the sensitivity of the instrument becomes much greater in the high pass filter mode, measurement of these two values provides a natural technique for inflight calibration of this sensitivity. This is performed by taking the difference between the two values and equating it to the sum of currents measured by the spectral mode within the difference range. It has also been found that the values in modes A and B are not obtained at equal sensitivity. The relative sensitivity between these values was obtained by studying an E region metallic layer in which the only heavy ion constituent of importance was iron (56^+). Since this could also be observed in the spectral mode, it was possible to ascertain that total mode A was approximately 1/4 as sensitive as total mode B. This relative sensitivity was assumed constant in the treatment of data at lower altitudes.

Applying the above relative sensitivity procedures to the high pass filter mode data, the composition was reduced to absolute values by using the total density data obtained from Gerdien and radio absorption experiments discussed in Paper 1. All masses were assigned equal weight in the normalization process, since the region under study is below altitudes where free molecular theory plays an important role. Mass dependent flow effects in

this transistion region are not well understood, but should gradually approach a very weak mobility type dependence at the lower altitudes.

POSITIVE ION COMPOSITION RESULTS

A. Shock Wave Effects

Figure 4 traces the raw current ratio of heavy constituents to total constituents during up and downleg of 14.424 as obtained from high pass filter mode data. An enhancement of this ratio thereby implies a greater contribution of heavy constituents to the total current. Of note is the uniform value of this ratio between up and downleg in the metallic region (90-100 km) where the major contribution to I_B is iron (56^+). The lack of change between up and downleg in this region suggests that the heavy constituents are either metallic atomic ions and hence unaffected by shock effects, or of another origin unperturbed by the relatively weak shocks there. Below 85 km, designated the water cluster region, an enhancement of nearly 10 is observed for the ratio, indicating a much greater contribution of heavy water cluster constituents in the wake sampling region than in that of the ram. These heavier clusters are known to have low energies of dissociation leading to the suggestion that shock wave temperature and pressure effects are sufficient to induce breakup of these heavier clusters to lighter clusters

(Narcisi, 1970; Narcisi and Roth, 1970). The evidence here appears to verify this suggestion because under ram conditions, sampling occurs much closer to that portion of the shock where ambient ions have been subjected to maximum pressures and temperatures. A certain percentage of such ions should also flow into the wake region, but a much higher proportion of particles sampled in the wake will have traversed across weaker portions of the shock at lower pressures, where conditions for dissociation are much less probable. Similar effects are also seen in the data of 14,425.

As shown in Figure 1, 14.425 traveled considerably slower than 14.424 in the water cluster domain. Comparison of either upleg or downleg data between the two flights indicates a higher proportion of heavy clusters (i.e. T_B in Figure 5 and 6) on the slower vehicle. The effect is not as apparent in the downleg individual constituent data of 14.425 because of a higher operating pressure ($\sim$ 50 times greater than on 14.424, cf. Table 2). This was induced by a reduced wake effect and lower pumping speed; the latter caused by cap ejection at a lower altitude on upleg. Data from previous flights on faster vehicles (Mach 6-7) through this region indicate that 19^+ and 37^+ are the only clusters remaining for sampling at such high velocities, even under wake sampling conditions.

Finally, the height of unit optical depth for Lyman alpha radiation, as measured aboard each payload with an EUV detector, is indicated on Figures 5 and 6. This height should provide the maximum concentration of NO^+. It is apparent, especially in the better quality data of Figure 6, that 48^+ and 55^+ peak near this height, suggesting that NO^+ has in fact gone into the production of these clusters (Ferguson and Fehsenfeld, 1969). This additional information provides consistency with the above conclusions, and suggests that wake sampled data at lower Mach numbers may be sufficiently reliable to represent the major qualitative features of D region composition and clustering.

B. Qualitative Features and Evaluation

The normalized positive ion composition profiles are illustrated in Figures 5 and 6 for 14.425 and 14.424, respectively. The curve marked T_B represents the sum of all mass to charge ratios for $M > 65$. In this work all ions are assumed to be singly ionized for identification purposes. T_B has been obtained from high pass filter mode data using sensitivity adjustments discussed earlier. It may thereby be in error by as much as a factor of two or three. The sum of all mass currents $46 < M < 66$ for 14.424 and $49 < M < 66$ for 14.425 have been deducted from I_B to obtain T_B values, in order to prevent double counting of masses within these ranges during the normalization process. The T_B curve shown is considered to be the best

possible representation of heavy mass ions from this data at the present time.

The sweep rate on both payloads provided a height resolution close to 1 km at D region altitudes. Some minor constituent data points are seen to be separated by much larger height intervals; missing points are absent because of their proximity to the extreme sensitivity limits of the instruments. The absence of NO^+ between 75 and 81 km on the upleg data of 14.425 is apparently real. All data shows a strong depletion of NO^+ below the Lyman alpha unit optical depth height. In this region the masses do not add up to the normalized profile because of the omission of sporadic trace constituents (probably of contaminent nature in this region of low sensitivity). Below 81 km, the data is sufficiently marginal to be treated on a qualitative rather than quantitative basis.

On both flights, the data cannot be read to accuracies better than $\pm$ 10% because of the logarithmic presentation necessitated to gain the broad sensitivity range desired. Other possible errors due to unknown corrections for relative mass flow, errors in the Gerdien and radio absorption data, and other factors imply error bars approaching $\pm$ 20% on the major constituents and $\pm$ 100% on the minor constituents, the latter value caused by the much stronger contribution of noise and other background effects to the small currents measured for these constituents. On both shots, the currents

measured below 75 km are very small, causing measurements to be made near the maximum sensitivity limits of the instrumentation. The large values shown are a result of the normalization and thought to be representative of the constituents present on a qualitative basis only. However, for the downleg portion of 14 421, the data may be quantitatively reliable to altitudes approaching 65 km.

On upleg, both flights indicated poor sensitivity up to 78 km although cap ejection occurred well below this height. On downleg, below the free molecular flow region (below 90 km), wake properties of the flow do not appear to reduce the quantities of ions reaching the spectrometer, as can be seen in Figure 3. Molecular non-cluster constituents (e.g. O_2^+, NO^+) are found to be present in the wake with similar mass ratios to those observed under ram conditions. The downleg enhanced values of the heavy cluster constituents (e.g. 48^+, 55^+) are opposite to those expected from free molecular flow or mobility effects, and suggest these enhancements to be a lower limit to those obtained with the anticipated small corrections from mass dependent considerations. The wake data is thereby important in providing data down to lower altitudes than obtainable from upleg ram, and in establishing the presence of certain constituents not observed in the ram configuration because of shock effects. Unfortunately, for 14.425, no downleg

data of any consequency was obtained below 75 km because of a loss of sensitivity related to a higher resolution setting coupled with higher operating pressures within the instrument.

From the previous discussion it is clear that modifications due to shock effects occur in the sampling of ion spectra with rocket-borne ion mass spectrometers. It is however, possible to develop a qualitative picture of the species and their distribution. A precise quantitative analysis will require ion mass spectrometer sampling at subsonic velocities.

The downleg ion density profiles from rocket 14.424 show the primary ion below 85 km to be 37^+ with 55^+ and 30^+ appearing as major ionic constituents. The hydronium ion, 19^+, as well as 48^+ are secondary. The distribution of 55^+ traces that of 30^+. In addition, the peaks of 55^+, 48^+, and 30^+ occur at 77 km, which is also the peak of production of NO^+ (30^+) by solar Lyman alpha radiation; this indicating that these ions originate from this ionization source. Above 83 km there is a sudden decrease in the hydrated ion cluster densities coinciding with the increase in electron density in the lower E region of the ionosphere.

The downleg data of 14.425 are not as good in quality as those of 14.424 because of higher operating pressures so that care should be taken in reading as much into the 14.425 profiles. It should be noted however, that in

this data 37^+ is no longer the dominant constituent; instead, 30^+ predominates. Ions of secondary importance are 37^+ and $M^+ > 65^+$.

INTERPRETATION AND DISCUSSION

In Paper 1 it was shown that the primary ionization sources were solar X-rays, galactic cosmic rays and ionization of nitric oxide. Therefore, to explain the observed ion distribution it is necessary to start with the ions formed by ionization of N_2 and O_2 as well as NO. The ion N_2^+ is rapidly converted to O_2^+ and NO^+ (to a certain extent) by the reactions of Table 3A. This implies that mechanisms must be found to produce hydrated ions from O_2^+ and NO^+.

A reaction sequence has been proposed that begins with O_2^+ and leads to 19^+, 37^+ and heavier clusters (Fehsenfeld and Ferguson, 1969; Ferguson and Fehsenfeld, 1969). This scheme is shown in Figure 7 with the reactions and rates detailed in Table 3B. The scheme requires the formation of O_4^+ and subsequent two-body reactions of the form

$$O_4^+ + H_2O \rightarrow O_2^+ \cdot H_2O + O_2 \quad (1)$$

$$O_2^+ \cdot H_2O + H_2O \rightarrow H_3O^+ + O_2 + OH \quad (2)$$

$$\rightarrow H_3O^+ \cdot OH + O_2 \quad (3)$$

$$H_3O^+ + H_2O + M \rightarrow H_3O^+ \cdot H_2O + M \quad (4)$$

together with the remaining reactions shown in Table 3B. Hydrates with mass greater than 37 are produced when 37^+ reacts with H_2O in a three body reaction. However, the predominant ion which must be transferred to hydrates is NO^+. This can be accomplished in an analogous way to O_4^+ formation by first forming the cluster ions $NO^+ \cdot O_2$, $NO^+ \cdot N_2$ and $NO^+ \cdot CO_2$. The rate coefficient for the reaction

$$NO^+ + CO_2 + N_2 \rightarrow NO^+ \cdot CO_2 + N_2 \qquad (5)$$

has been measured to be 2.5×10^{-29} $cm^6 sec^{-1}$ at D region temperatures, Dunkin et al (1971). In addition, they have placed upper limits of 5×10^{-33} $cm^6 sec^{-1}$ and 2×10^{-32} $cm^6 sec^{-1}$ for $NO^+ \cdot N_2$ and $NO^+ \cdot O_2$ formation with He and Ar as third bodies but not O_2 and N_2. Predictions based on polarizability by Heimerl and Puckett (1971) and Beyer and Keller (1971) would indicate larger rate coefficients for $NO^+ \cdot O_2$ and $NO^+ \cdot N_2$ then the upper limit set by Dunkin et al. The D region ion density data require a value of 6×10^{-32} $cm^6 sec^{-1}$ for reaction between NO^+ and its clustering neutral, where the neutral bodies of the reaction are each total neutral particle density. The mesospheric CO_2 concentration is unknown but an estimate of the number density mixing ratio is 3×10^{-4}, (Hays and Olivero, 1970). This would give 9×10^{-33} $cm^6 sec^{-1}$ for the equivalent CO_2 clustering rate, but this is insufficient to explain the data of 14.424 and would require either a

larger rate coefficient or contributions from molecules other than CO_2. However one must bear in mind that part of the problem lies with the data itself, in obtaining absolute number densities of specific ambient ions from D region ion mass spectrometers at supersonic speeds.

The ion $NO^+ \cdot CO_2$ transfers to $NO^+ \cdot H_2O$ by the reaction

$$NO^+ \cdot CO_2 + H_2O \rightarrow NO^+ \cdot H_2O + CO_2 \qquad (6)$$

There is a continued reaction with water until (see table 3A)

$$NO^+ \cdot (H_2O)_3 + H_2O \rightarrow H_3O^+ \cdot (H_2O)_2 + HNO_2 \qquad (7)$$

occurs as shown in Figure 7. The ions 19^+ and 37^+ are not formed in this reaction sequence; rather ions such as 55^+, 73^+, and heavier hydrates occur. Since the principal ion observed is 37^+, it might be argued that this ion is formed by shock wave fragmentation of the heavier hydrates. However, there is a difficulty with the reaction scheme in that the three body reactions involved in the chain leave most of the ions as 48^+ rather than as hydrates of greater mass.

A way out of the difficulty can be achieved by use of a reaction postulated by Burke (1970). The reaction

$$NO^+ \cdot H_2O + H \rightarrow H_3O^+ + NO \qquad (8)$$

should be exothermic although it has not been observed thus

far in the laboratory. The effect of including this reaction is shown in Figure 8. Here the 37^+ distribution is shown as a function of rate coefficient for (8). The distribution of 73^+ is also shown. The concentration of hydrated ions below 80 km is a sensitive function of (8). Above 80 km 37^+ is controlled by O_2^+ and N_2^+ production as shown in Figure 8 for the case of no O_2^+ and N_2^+ sources.

In paper 1 it was shown that the "effective recombination coefficient", derived from the measured electron density profiles and Meira's (1971) nitric oxide distribution, was consistent with the laboratory measurements of the dissociative recombination rate of hydrated ions with electrons. These rates of reaction are now combined with the Meira NO distribution and the reactions in Table 3 using the total density as the third body, M, to predict the altitude distribution of ion composition in the D region. It is assumed that the negative ion to electron ratio is less than unity at all altitudes above 70 km so that the primary loss process for ions and electrons is dissociative recombination. A zenith angle of 27.8^o corresponding to that of 14.424 is assumed. The distribution of neutral atomic oxygen used is approximately that of Shimazaki and Laird (1970). The neutral water content is taken to be 4 ppm. Some of the clustering reaction rates have an inverse temperature dependence (Bohme et al., 1969) which has not been considered here.

The results of the above calculation are illustrated in Figure 9. The predicted 37^+ distribution is dominant but less in magnitude than that observed The calculations predict an increase in the concentration of heavy hydrate ions such as 73^+ at lower altitudes, not observed in these flights because of sweep range limitations but found on subsequent flights. Additional computations show that the apparent reduction of 37^+ to secondary status in the data of 14.425 is explained above 80 km by the reduced O_2^+ and N_2^+ production with larger zenith angle. However this would not account for the absence of 37^+ below 80 km. If the Burke mechanism is operative, hydrates would be expected at lower altitudes even for larger zenith angles

The sharp cutoff of 37^+ at higher altitudes is governed by the reaction

$$O_4^+ + O \rightarrow O_3^+ + O_2 \qquad (9)$$

competing at higher altitudes with reaction (1). It is therefore quite sensitive to the concentration of atomic oxygen.

Finally, the observed water cluster light ion distribution (19^+, 37^+) under wake sampling conditions must contain an unknown percentage of shock dissociated cluster ions in addition to the ambient contributions. This implies the measured distributions of 19^+ and 37^+ to be an upper limit

for the ambient distribution of such ions, although more nearly correct than values obtained under ram sampling.

CONCLUSIONS

D region positive ion composition profiles for two solar zenith angles (27.8^{o} and 53.2^{o}) have been measured and normalized to absolute values with the aid of simultaneous positive ion and electron density measurements. Strong evidence for the modification of the ambient distribution by the shock wave under ram sampling conditions is presented, leading to the conclusion that wake data is more reliable for proper sampling. The ram shock is found to be responsible for the dissociation of heavy water clusters, e.g. $H_3O^+ \cdot (H_2O)_n$, into lighter clusters dominated by n = 1. Heavy clusters, i.e. $n \geq 2$, are found in much greater abundance in the wake region where shock effects due to temperature and pressure increases should be less severe.

Under the assumption that wake composition data is more closely representative of the ambient distribution than ram sampled data, certain qualitative features are immediately apparent. The 37^+ cluster ion is found to dominate the distribution for $\chi = 27.8^{o}$, but reduces to secondary importance for $\chi = 53.2^{o}$, suggesting X-ray ionization control, at least above 80 km. Water cluster constituents 48^+, 55^+, and $M^+ > 65$ are found to peak near

the height of Lyman α unit optical depth, suggesting clustering chemistry involving NO^+ for the formation of these constituents. An apparent depletion of NO^+ below this height further enhances this argument. A severe cutoff of water clusters is observed to occur between 80 and 85 km, coincident with a strong positive gradient in electron density.

The wake ion composition profiles together with simultaneous measurements of Lyman alpha radiation and X-ray flux are used to evaluate ion clustering schemes for the conversion of NO^+ and O_2^+ into hydrated cluster ions. The ion-pair production function is based on neutral nitric oxide concentrations consistent with recently reported measurements by Meira (1971), together with ionization of O_2 and N_2. It is shown that the O_2^+ clustering scheme is effective in producing $37^+(H_3O^+ \cdot H_2O)$ above 80 km.

Concentrations of NO^+, $NO^+ \cdot H_2O$, $H_3O^+ \cdot (H_2O)_2$ and heavier hydrates require a rate coefficient for the clustering reaction

$$NO^+ + X + M \rightarrow NO^+ \cdot X + M \qquad (10)$$

which is greater than has been measured in the laboratory thus far for X being CO_2, N_2 or O_2. It has also been necessary to employ the reaction

$$NO^+ \cdot H_2O + H \rightarrow H_3O^+ + NO \qquad (11)$$

which is currently not verified by laboratory measurements.

Much additional laboratory work is necessary before clustering can be accepted as the origin of D region hydrated ions. The rates of many reactions must be determined before theoretical and experimental results can agree quantitatively. It is apparent that the D region positive ion composition is extremely sensitive not only to the primary ions produced (NO^+, O_2^+, N_2^+) but also to minor neutral constituents such as NO, H_2O, O, CO_2 and E.

On the experimental side, explicit measurements of heavy hydrates will require mass spectrometers sweeping to higher mass number under subsonic conditions. Only after these steps have been taken can the true positive ion composition of the D region be established quantitatively.

ACKNOWLEDGEMENT

This program was successfully completed through the diligent efforts of the technical staff assigned to the Chemosphere Branch for direct support of this work. In particular, we wish to thank Mr. Donald Silbert for his contributions to the technical development of the quadrupole ion mass spectrometer and associated systems for application to this work. Messrs. Roy Hagemeyer and Giles Spaid were largely responsible for the radio wave absorption experiment. We wish to thank members of the Goddard Sounding Rocket Division for the many services they performed including introduction of tone ranging to determine trajectory. The assistance of John Jackson in the trajectory analysis is greatly appreciated. We also wish to thank the Indian Launch Range (TERLS) under the directorship of Mr. H.G.S. Murthy, for their excellent cooperation and support.

REFERENCES

Aikin, A.C., R.A. Goldberg, and Y.V. Somayajulu, "Electron and Positive Ion Density Altitude Distribution in the Equatorial D Region", to be published in 1971.

Beyer, R.A. and G.E. Keller, "The Clustering of Atmospheric Gases to Alkali Ions", Trans. Am. Geophys. Union, 52, No. 4, (1971).

Biondi, M.A., "Electron-ion and Ion-ion Recombination", Ann. Geophys., 20, 34, 1964.

Biondi, M.A., private communication.

Bohme, D.K., D.B. Dunkin, F.C. Fehsenfeld and E.E. Ferguson, "Flowing Afterglow Studies on Ion-molecule Associative Reactions", J. Chem. Phys., 51, 863-872, 1969.

Burke, R.R., "Hydrogen Atom Participation in D Region Ion Chemistry", J. Geophys. Res., 75, 1345-1347, 1970.

Durden, D.A., P. Kebarle, and A. Good, "Thermal Ion-molecule Reaction Rate Constants at Pressures up to 10 torr with a Pulsed Mass Spectrometer. Reactions in Methane, Krypton and Oxygen", J. Chem. Phys., 50, 805-813, 1969.

Dunkin, D.B., F.C. Fehsenfeld, A.L. Schmeltkopf and E.E. Ferguson, "Three-body Association Reactions of NO^+ with O_2, N_2 and CO_2", J. Chem. Phys., in press.

Fehsenfeld, F.C., M. Moseman and E.E. Ferguson, "Ion-molecule Reactions in an $NO^+ \cdot H_2O$ System", J. Chem. Phys., in press, a.

Fehsenfeld, F.C., M. Moseman and E.E. Ferguson, "Ion-molecule Reactions in an $O_2^+ \cdot H_2O$ System", J. Chem. Phys., in press, b.

Fehsenfeld, F.C., D.B. Dunkin and E.E. Ferguson, "Rate Constants for the Reaction of CO_2^+ with O, O_2 and NO; N_2^+ with O and NO; and O_2^+ with NO", Planetary Space Sci , 18, 1267-1269, 1970.

Fehsenfeld, F.C. and E.E. Ferguson, "Origin of Water Cluster Ions in the D Region", J. Geophys. Res., 74, 2217-2222, 1969.

Fehsenfeld, F.C., A.L. Schmeltkopf and E.E. Ferguson, "Some Measured Rates of Oxygen and Nitrogen Ion-molecule Reactions of Atmospheric Importance Including $O^+ + N_2 \rightarrow NO^+ + N$", Planetary Space Sci., 13, 219-223, 1965.

Ferguson, E.E., private communication, 1970.

Ferguson, E.E. and F.C. Fehsenfeld, "Water Vapor Ion Cluster Concentrations in the D Region", J. Geophys. Res., 74, 5743-5751, 1969.

Ferguson, E.E., F.C. Fehsenfeld, P.D. Goldan and A.L. Schmeltkopf, "Positive Ion-neutral Reactions in the Ionosphere", J. Geophys. Res., 70, 4323-4329, 1965.

Goldberg, R.A. and L.J. Blumle, "Positive Ion Composition from a Rocket-Borne Mass Spectrometer", J. Geophys. Res., 75, 133-142, 1970.

Good, A., D.A. Durden and P. Kebarle, "Ion-molecule Reactions in Pure Nitrogen and Nitrogen Containing Traces of Water at Total Pressures of 0.5-4 torr. Kinetics of Clustering Reactions Forming $H^+ \cdot (H_2O)_n$", J. Chem. Phys., 52, 212-221, 1970.

Hays, P.B. and J.J. Olivero, "Carbon Dioxide and Monoxide above the Troposphere", Planetary Space Sci., 18, 1729-1733, 1970.

Heimerl, J. and L.J. Puckett, "$NO^+ \cdot CO_2$ Clusters as an Intermediate Lending to the Formation of Hydrated Hydronium in the D Region", Trans. Am. Geophys. Union, 52, No. 4, 1971.

Howard, C.J., H.W. Rundle and F. Kaufman, "Rates of Formation of Water Clusters for O_2^+ and NO^+", 23rd Annual Gaseous Electronics Conference, Oct. 23, 1970, Hartford, Conn., Bull. Am. Phys. Soc., 16, 213, 1971.

Huffman, R.E., D.E. Paulsen, J.C. Larrabee and R.B. Cairns, "Decrease in D-Region $O_2(^1\Delta_g)$ Photionization Rates Resulting from CO_2 Absorption", J. Geophys. Res., 76, 1028-1038, 1971.

Hunt, W.W., Jr., "Meteorological and Chemical Factors in D-Region Aeronomy", Record 3rd Aeronomy Conference, Aeronomy Rept. No. 32, p. 311, ed. by C.F. Sechrist, Jr., Univ. of Illinois, Urbana, Illinois, 1969.

Hunten, D.M. and M.B. McElroy, "Metastable $O_2(^1\Delta_g)$ as a Major Source of Ions in the D-Region", J. Geophys. Res., 73, 2421, 1968.

Kasner, W.H. and M.A. Biondi, "Temperature Dependence of the Electron-O_2^+ Ion Recombination Coefficient", Phys. Rev., 174, 139, 1968.

Meira, L.G., Jr., "Rocket Measurements of Upper Atmospheric Nitric Oxide and Their Consequences to the Lower Ionosphere", J. Geophys. Res., 76, 202-212, 1971.

Narcisi, R.S., "Ion Composition Measurements and Related Ionospheric Processes in the D and Lower E Region", Ann. Geophys., 22, 224, 1966.

Narcisi, R.S., "Ion Composition in the Mesosphere", Space Research, VII, 186-196, ed. by R.L. Smith-Rose, North Holland Publishing Co., 1967.

Narcisi, R.S., "On Water Cluster Ions in the Ionospheric D Region", Planetary Electrodynamics, 2, ed. by S.C. Coroniti and J. Hughes, Gordon and Breach, New York, 1969.

Narcisi, R.S., "Shock Wave and Electric Field Effects in D Region Water Cluster Ion Measurements", Trans. Am. Geophys. Union, 51, No. 4, April 1970.

Narcisi, R.S. and A.D. Bailey, "Mass Spectrometric Measurements of Positive Ions at Altitudes from 64 to 112 Kilometers", J. Geophys. Res., 70, 3687-3700, 1965.

Narcisi, R.S. and W. Roth, "The Formation of Cluster Ions in Laboratory Sources and in the Ionosphere", Advances in Electronics and Electron Physics, 29, pp. 79-113, Academic Press Inc., New York, 1970.

Nicolet, M. and A.C. Aikin, "The Formation of the D Region of the Ionosphere", J. Geophys. Res., 65, 1469-1483, 1960.

Puckett, L.J. and M.W. Teague, "Production of $H_3O^+ \cdot nH_2O$ from NO^+ Precursor in NO-H_2O Gas Mixtures", J. Chem. Phys., 54, 2564-2572, 1971.

Shimazaki, T. and A.R. Laird, "A Model Calculation of the Diurnal Variation in Minor Neutral Constituents in the Mesosphere and Lower Thermosphere Including Transport Effects", J. Geophys. Res., 75, 3221-3235, 1970.

Swider, W., "Sources for $H_3O^+ \cdot (H_2O)_n$ Ions in the D Region", J. Geophys. Res., 75, 7299-7300, 1970.

Warneck, P., "Laboratory Rate Coefficients for Positive Ion-molecule Reactions in the Ionosphere", J. Geophys. Res., 72, 1651-1653, 1967.

Weller, C.S. and M.A. Biondi, "Recombination Attachment and Ambipolar Diffusion of Electrons in Photoionized NO Afterglows", Phys. Rev., 172, 198, 1968.

LIST OF TABLES

TABLE 1

PARAMETER	NASA 14.425	NASA 14.424
Date	3/19/70	3/19/70
Launch Time (LMT)	8:27	10:17
Solar Zenith Angle	53.2°	27.8°
Payload Weight	137 lb.	130 lb.
Spin Rate	5.9 c/s	7.9 c/s
Coning Angle	$< \pm 10^{\circ}$	$< \pm 1^{\circ}$
Coning Period	2.8 sec	1.5 sec
Trajectory Azimuth (Clockwise from North)	267°	259°
Payload Aspect		
Azimuth	275°	256.3°
Elevation	71.4°	72.9°
Apogee Altitude	100.8 km	121.9 km
Range Location		
Latitude		8.53° North
Longitude		76.95° East
Magnetic Dip		-1.7°

TABLE 2

Characteristic	14.425	14.424
Entrance Aperture Diameter	0.020 in.	0.020 in
Rod Length	4 in.	4 in.
Sampling Interval	1.25 sec.	1.29 sec.
Sweep Range	4-66 AMU	5-66 AMU
Mass Range (High pass filter mode, T_B)	>49 AMU	>46 AMU
Time/Unit Mass	0.016 sec.	0.017 sec.
RF Frequency	2.85 MHz	2.85 MHz
Attractive Potential	- 10 volts	- 10 volts
Mean Operating Pressure at 75 to 85 km (as measured by triode ion pump)		
Upleg	7.4×10^{-5} torr	9×10^{-5} torr
Downleg	5×10^{-5} torr	1.2×10^{-6} torr

TABLE 3 A

REACTION	RATE USED	LAB. RATE	REFERENCE
$N_2^+ + O_2 \rightarrow O_2^+ + N_2$	1.0(-10)	1.0(-10)	Fehsenfeld et al (1965) Warneck (1967)
$N_2^+ + O \rightarrow NO^+ + N$	1.4(-10)	1.4(-10)	Fehsenfeld et al (1970)
$N_2^+ + e \rightarrow N + N$	4.0(-7)	4.0(-7)	Biondi (1964)

NOTE: Reaction rate units - $cm^3 sec^{-1}$

TABLE 3B

REACTION	RATE USED	LAB. RATE	REFERENCE
$O_2^+ + O_2 + M \rightarrow O_4^+ + M$	5(-30)	2.8(-30)	Durden et al (1969)
$O_4^+ + H_2O \rightarrow O_2^+ \cdot H_2O + O_2$	2.2(-9)	2.2(-9)	Fehsenfeld et al (1971b)
$O_2^+ \cdot H_2O + H_2O \rightarrow H_3O^+ + OH + O_2$	3.0(-10)	3.0(-10)	Fehsenfeld et al (1971b)
$\rightarrow H_3O^+ \cdot OH + O_2$	1.9(-9)	1.9(-9)	Fehsenfeld et al (1971b)
$H_3O^+ \cdot OH + H_2O \rightarrow H_3O^+ \cdot H_2O + OH$	5.0(-9)	3.0(-9)	Fehsenfeld et al (1971b)
$H_3O^+ + H_2O + M \rightleftarrows H_3O^+ \cdot (H_2O) + M$	9(-27)	3.4(-27)	Good et al (1970)
	7(-26)	7.0(-26)	
$H_3O^+ \cdot H_2O + H_2O + M \rightleftarrows H_3O^+ \cdot (H_2O)_2 + M$	2.3(-27)	2.3(-27)	Good et al (1970)
	7.0(-18)	7.0(-18)	
$H_3O^+ \cdot (H_2O)_2 + H_2O + M \rightleftarrows H_3O^+ \cdot (H_2O)_3 + M$	2(-27)	2.4(-27) 3.5(-27)	Good et al (1970) Puckett & Teague (1971)
	4(-14)	4.0(-14) 1.3(-14)	Good et al (1970) Puckett & Teague (1971)
$O_2^+ + H_2O + M \rightarrow O_2^+ \cdot H_2O + M$	4(-28)	2.8(-28)	Fehsenfeld et al (1971b)
$O_2^+ \cdot H_2O + H \rightarrow H_3O^+ + O_2$	1(-9)	no value	
$O_4^+ + O \rightarrow O_2^+ + O_3$	1(-10)	1(-10)	Ferguson, private communication
$O_2^+ + NO \rightarrow NO^+ + O_2$	8(-10)	8(-10)	Ferguson et al (1965) Warneck (1967)
$O_2^+ + e \rightarrow O + O$	3(-7)	3(-7)	Kasner & Biondi (1968)
$O_4^+ + e \rightarrow$ neutrals	2.3(-6)	2.3(-6)	Kasner & Biondi (1968
$O_2^+ \cdot H_2O + e \rightarrow$ neutrals	8(-6)	no value	
$H_3O^+ + e \rightarrow$ neutrals	2.5(-6)	1.3(-6) *	Biondi, private communication
$H_3O^+ \cdot (H_2O) + e \rightarrow$ neutrals	5(-6)	2.7(-6) *	
$H_3O^+ \cdot (H_2O)_2 + e \rightarrow$ neutrals	8(-6)	4.6(-6) *	
$H_3O^+ \cdot (H_2O)_3 + e \rightarrow$ neutrals	8(-6)	no value	

NOTES:
1) Three body reaction rate units - $cm^6 sec^{-1}$
2) Two body reaction rate units - $cm^3 sec^{-1}$
3) For reversible reactions - upper rate and lower rate refer to forward and reverse directions, respectively
4) Unless otherwise stated, M refers to N_2 for laboratory measurements

* Measured at 300^oK

TABLE 3C

REACTION	RATE USED	LAB. RATE	REFERENCE
$NO^+ + CO_2 + N_2 \rightarrow NO^+ \cdot CO_2 + N_2$		2.5±1.5(-29)	
$NO^+ + CO_2 + Ar \rightarrow NO^+ \cdot CO_2 + Ar$		3.5±1 (-29)	
$NO^+ + N_2 + He \rightarrow NO^+ \cdot N_2 + He$	6(-32)	<5(-33)	Dunkin et al (1971)
$NO^+ + O_2 + He \rightarrow NO^+ \cdot O_2 + He$		<6(-34)	
$NO^+ + O_2 + Ar \rightarrow NO^+ \cdot O_2 + Ar$		<2(-32)	
$NO^+ + H_2O + M \rightarrow NO^+ \cdot H_2O + M$	3(-28)	1.6(-28)	Howard et al (1971)
		1.4(-28)	Fehsenfeld et al (1971a)
$NO^+ \cdot CO_2 + H_2O \rightarrow NO^+ \cdot H_2O + CO_2$	1(-9)	~ 1(-9)	Dunkin et al (1971)
$NO^+ \cdot H_2O + H_2O + M \rightleftarrows NO^+ \cdot (H_2O)_2 + M$	1(-27)	1.0(-27)	Fehsenfeld et al (1971a)
	1(-13)	<1.0(-13)	
$NO^+ \cdot (H_2O)_2 + H_2O + M \rightleftarrows NO^+ \cdot (H_2O)_3 + M$	2(-27)	2.0(-27)	Fehsenfeld et al (1971a)
	1.3(-12)	1.3(-12)	
$NO^+ \cdot (H_2O)_3 + H_2O \rightarrow H_3O^+ \cdot (H_2O)_2 + HNO_2$	8(-11)	8(-11)	Fehsenfeld et al (1971a)
$NO^+ \cdot H_2O + H \rightarrow H_3O^+ + NO$	1(-9)	no value	
$NO^+ + e \rightarrow N + O$	7(-7)	7.4(-7)	Weller & Biondi (1968)
$NO^+ \cdot M + e \rightarrow$ neutrals	8(-6) *	no value	
$NO^+ \cdot (H_2O)_n + e \rightarrow$ neutrals	8(-6) **	no value	

NOTES:
1) Three body reaction rate units - $cm^6 sec^{-1}$
2) Two body reaction rate units - $cm^3 sec^{-1}$
3) For reversible reactions - upper rate and lower rate refer to forward and reverse directions, respectively
4) Unless otherwise stated, M refers to N_2 for laboratory measurements

* M is CO_2, N_2 or O_2

** n = 1, 2, 3

FIGURE CAPTIONS

Figure 1 - Velocity profile of 14.425 and 14.424 in terms of Mach number.

Figure 2 - Front end payload configuration during flight. The spectrometer cap is ejected prior to data sampling.

Figure 3 - Typical up and downleg raw spectra obtained from the ion mass spectrometer aboard 14.424.

Figure 4 - Current ratios indicating the relative contribution of heavy ionic constituents to the total current sampled.

Figure 5 - The absolute ion composition distribution from 14.425 data.

Figure 6 - The absolute ion composition distribution from 14.424 data.

Figure 7 - The reaction sequence employed for theoretical calculations.

Figure 8 - The altitude distribution of 37^+ and 73^+ for different rates (k) of the reaction $NO^+ \cdot H_2O + H \rightarrow H_3O^+ + NO$. The altitude distribution for 37^+ when no sources of O_2^+ and N_2^+ production are included is indicated by o---o. This computation is made for $k = 10^{-9}$ cm^3 sec^{-1}.

Figure 9 - Predicted ion distribution for $\chi = 27.8^o$.

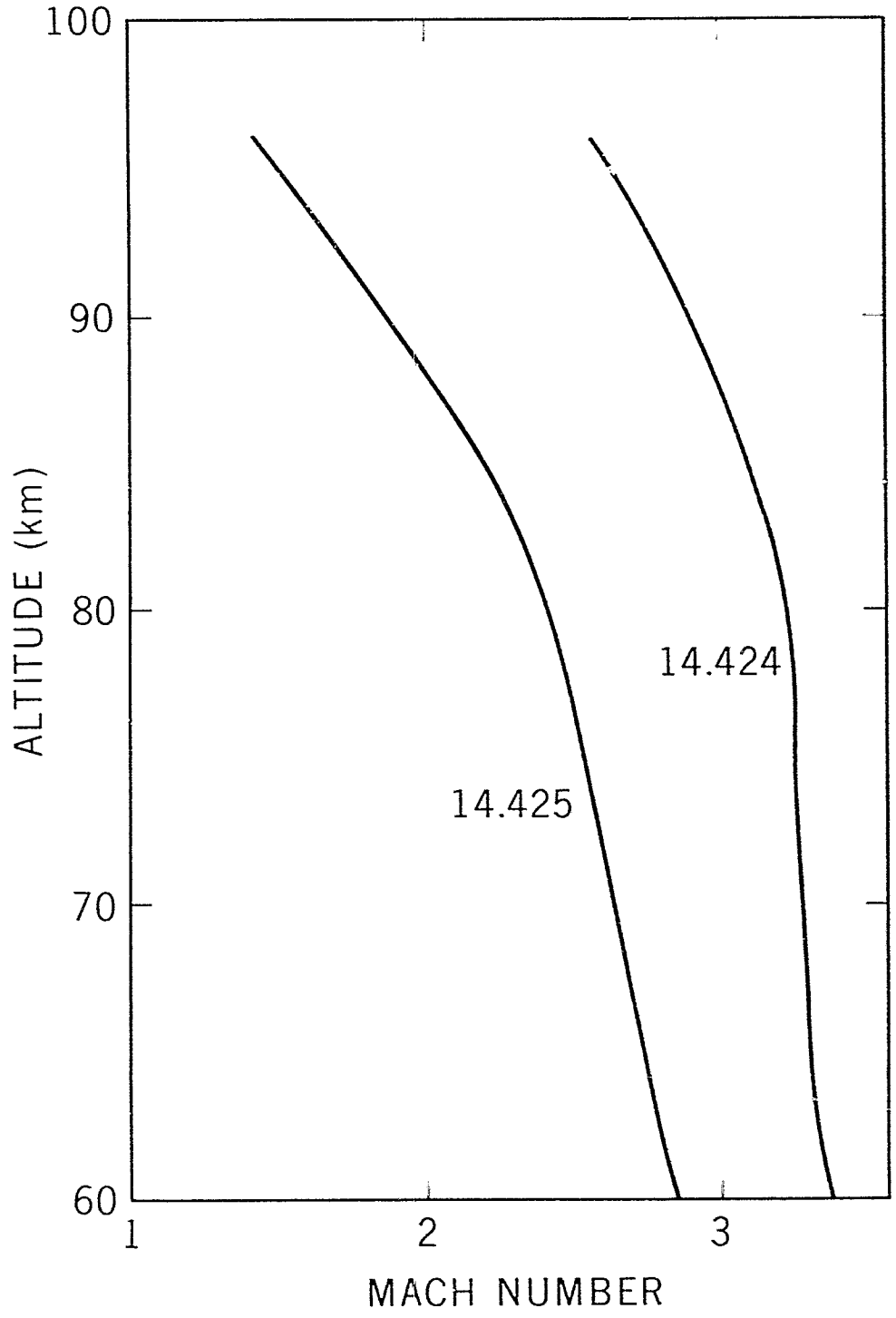

Figure 1

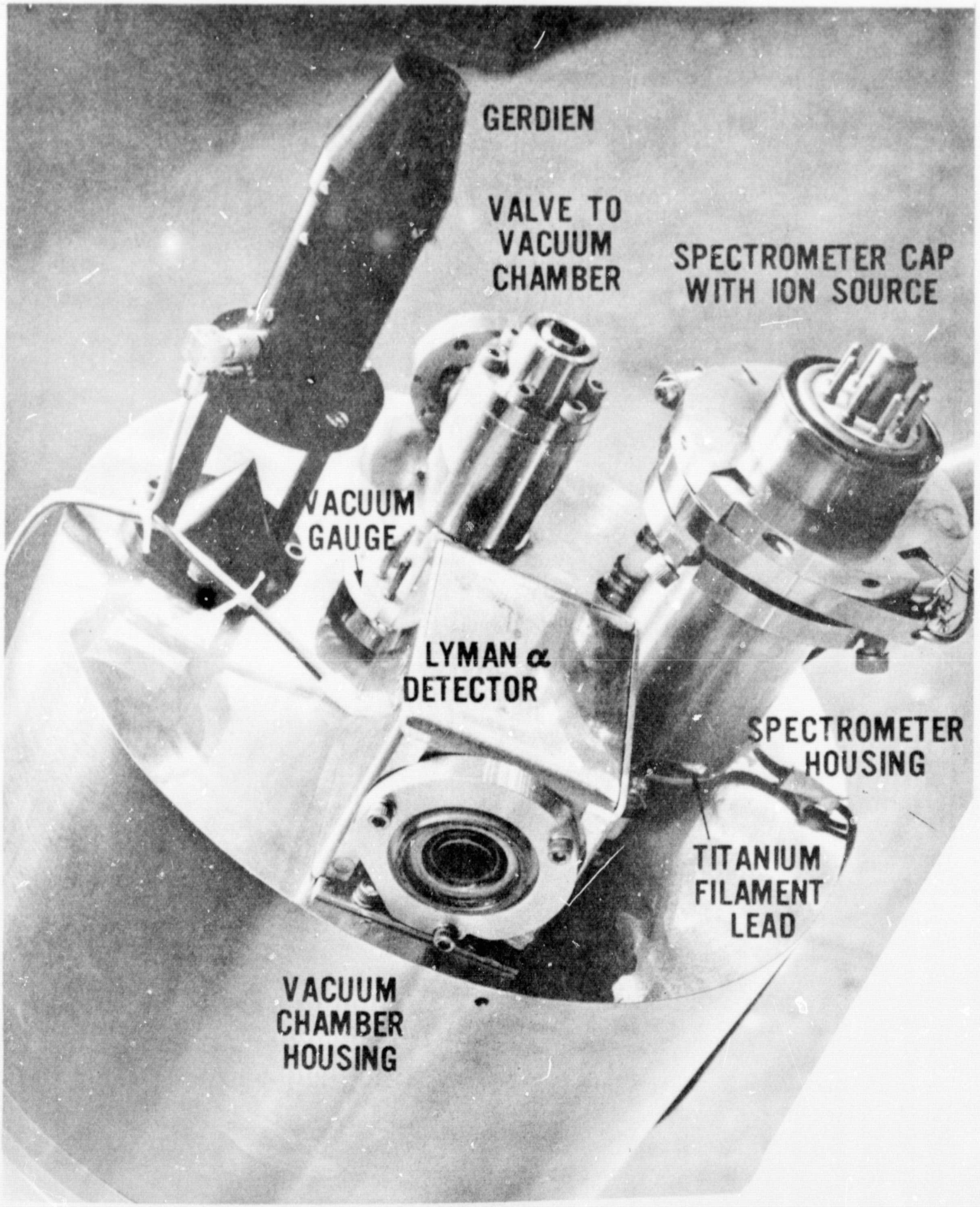
GERDIEN
VALVE TO VACUUM CHAMBER
SPECTROMETER CAP WITH ION SOURCE
VACUUM GAUGE
LYMAN α DETECTOR
SPECTROMETER HOUSING
TITANIUM FILAMENT LEAD
VACUUM CHAMBER HOUSING

Figure 2

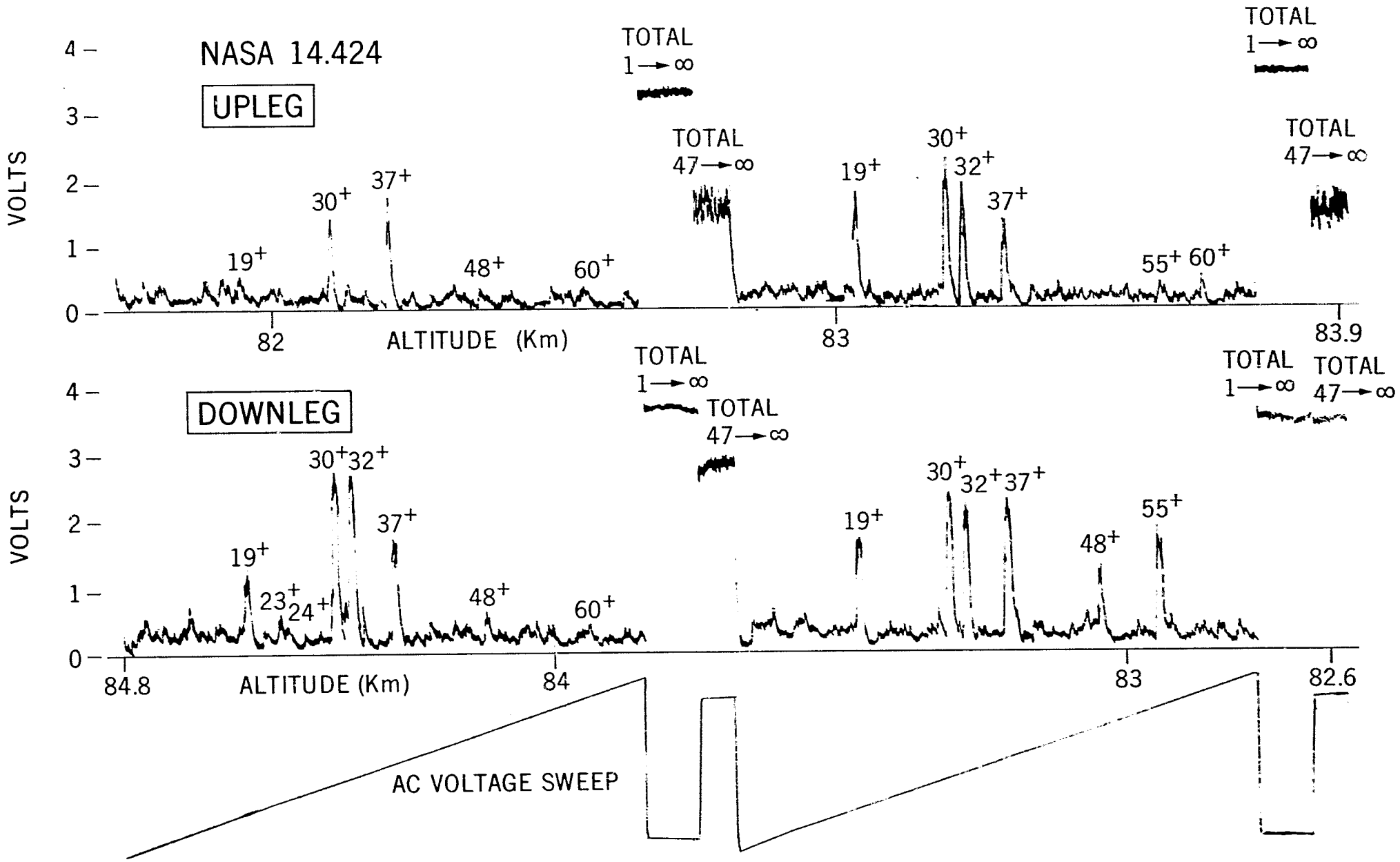
NASA 14.424
UPLEG
DOWNLEG
VOLTS
4
3
2
1
0
19+
30+
37+
48+
60+
82
ALTITUDE (Km)
83
83.9
TOTAL 1→∞
TOTAL 47→∞
55+
32+
23+
24+
84.8
84
82.6
AC VOLTAGE SWEEP

Figure 3

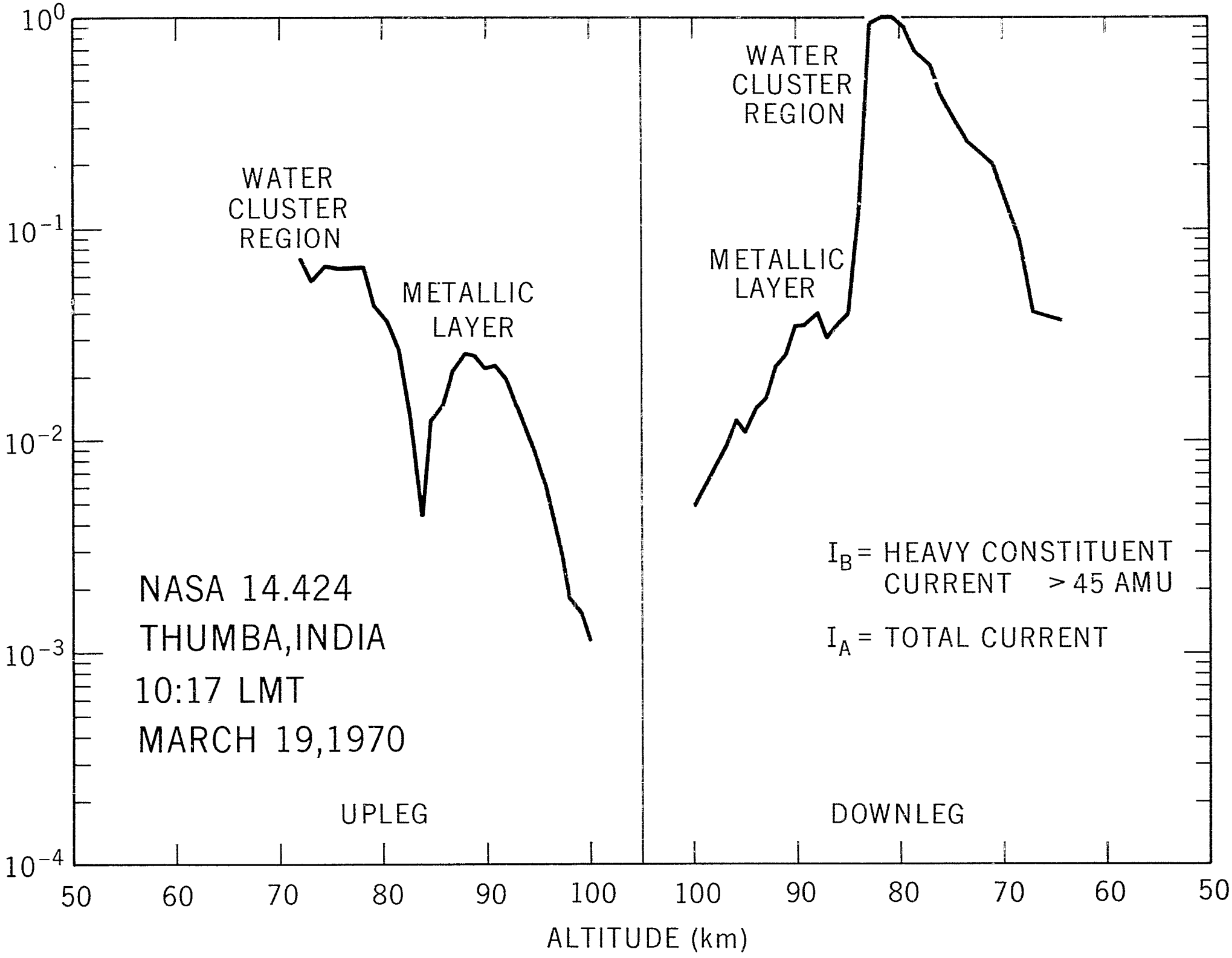
10^0
10^{-1}
10^{-2}
10^{-3}
10^{-4}
I_B/I_A
WATER CLUSTER REGION
METALLIC LAYER
NASA 14.424
THUMBA,INDIA
10:17 LMT
MARCH 19,1970
WATER CLUSTER REGION
METALLIC LAYER
I_B = HEAVY CONSTITUENT CURRENT > 45 AMU
I_A = TOTAL CURRENT
UPLEG
DOWNLEG
50 60 70 80 90 100 100 90 80 70 60 50
ALTITUDE (km)

Figure 4

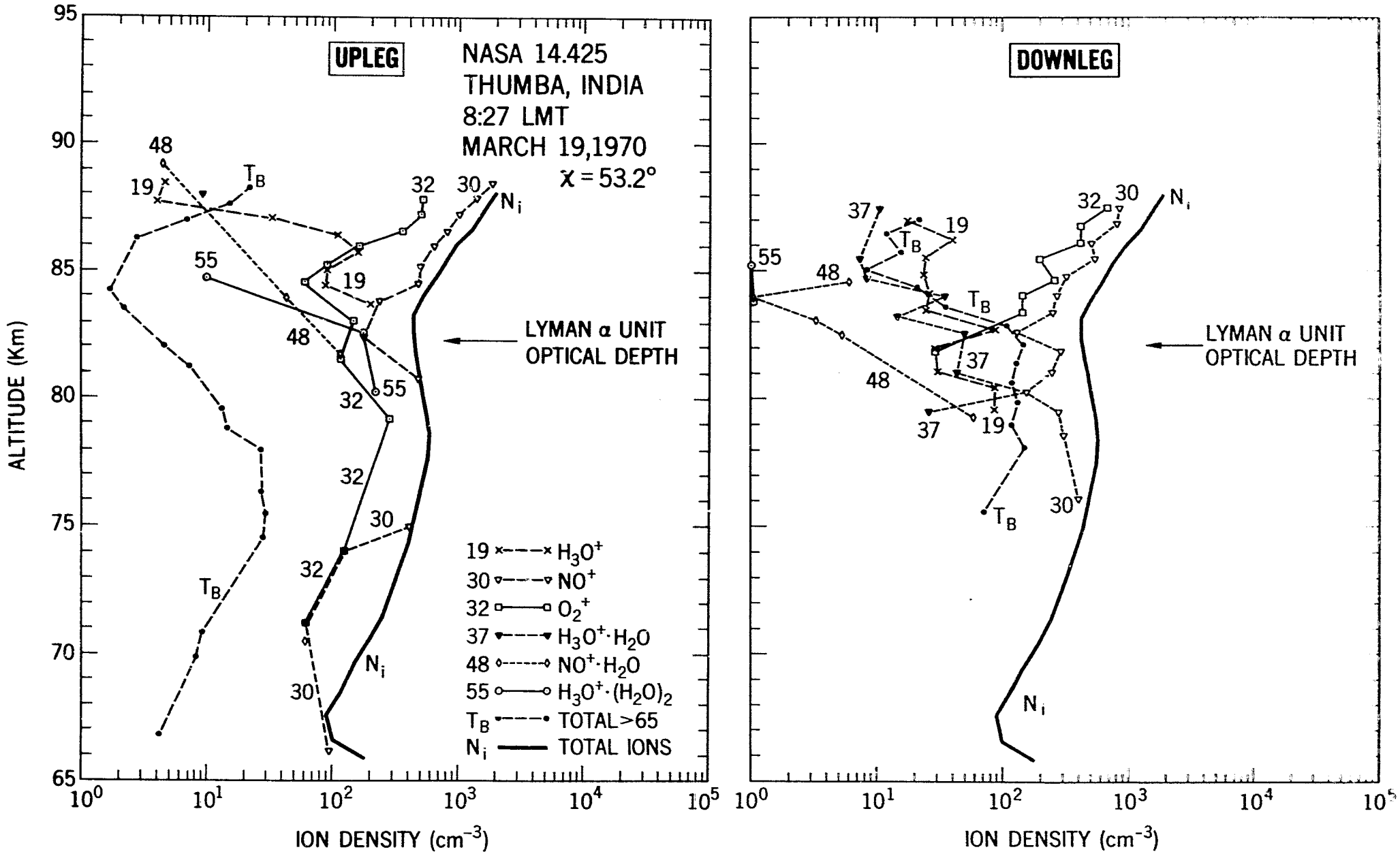
UPLEG
NASA 14.425
THUMBA, INDIA
8:27 LMT
MARCH 19,1970
χ = 53.2°
DOWNLEG
LYMAN α UNIT
OPTICAL DEPTH
ALTITUDE (Km)
ION DENSITY (cm⁻³)
19 H3O+
30 NO+
32 O2+
37 H3O+·H2O
48 NO+·H2O
55 H3O+·(H2O)2
TB TOTAL>65
Ni TOTAL IONS

Figure 5

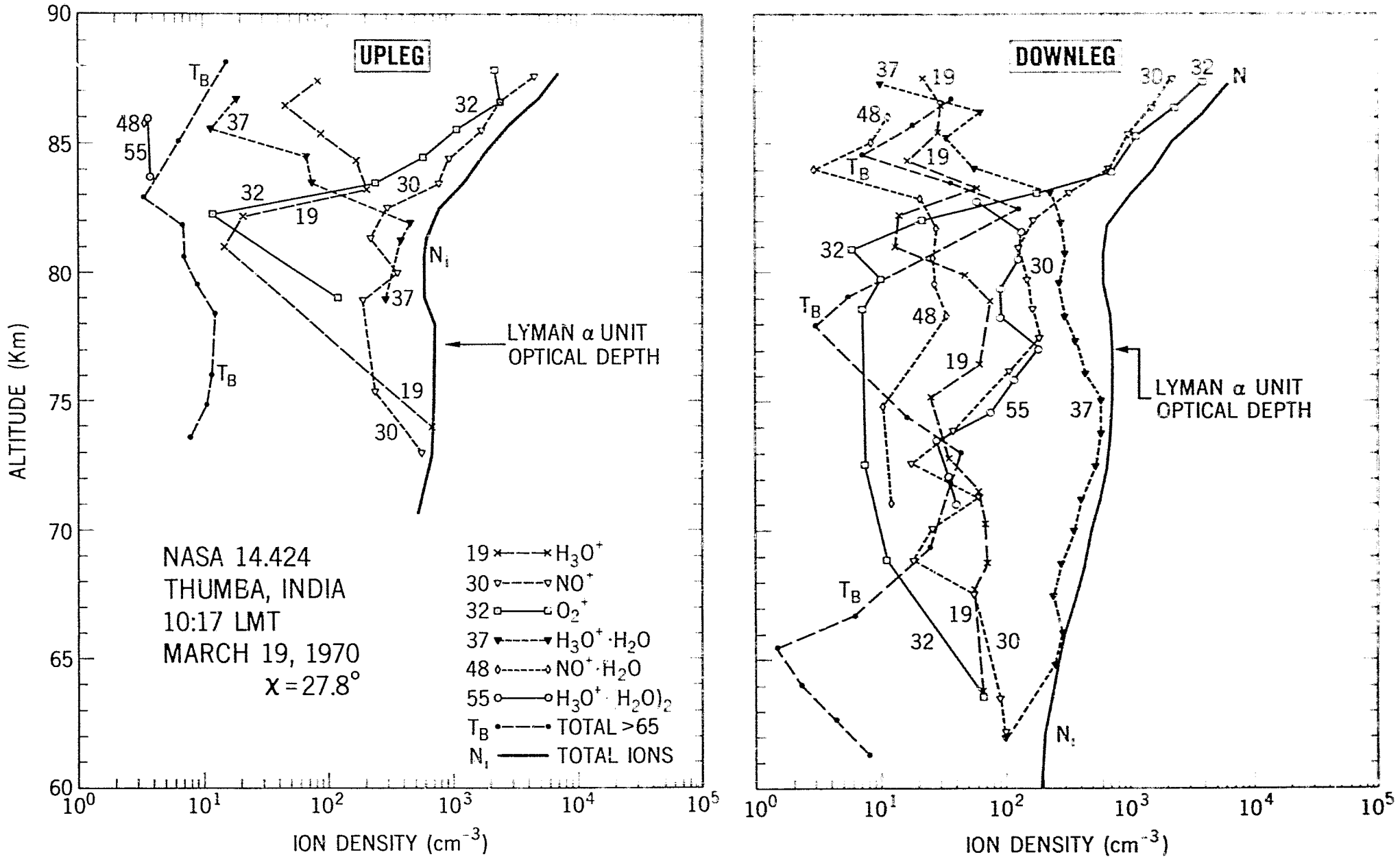
UPLEG
DOWNLEG
ALTITUDE (Km)
ION DENSITY (cm^{-3})
LYMAN α UNIT OPTICAL DEPTH
N_i
T_B
NASA 14.424
THUMBA, INDIA
10:17 LMT
MARCH 19, 1970
χ = 27.8°
19 H_3O^+
30 NO^+
32 O_2^+
37 $H_3O^+ \cdot H_2O$
48 $NO^+ \cdot H_2O$
55 $H_3O^+ \cdot (H_2O)_2$
T_B TOTAL >65
N_i TOTAL IONS

Figure 6

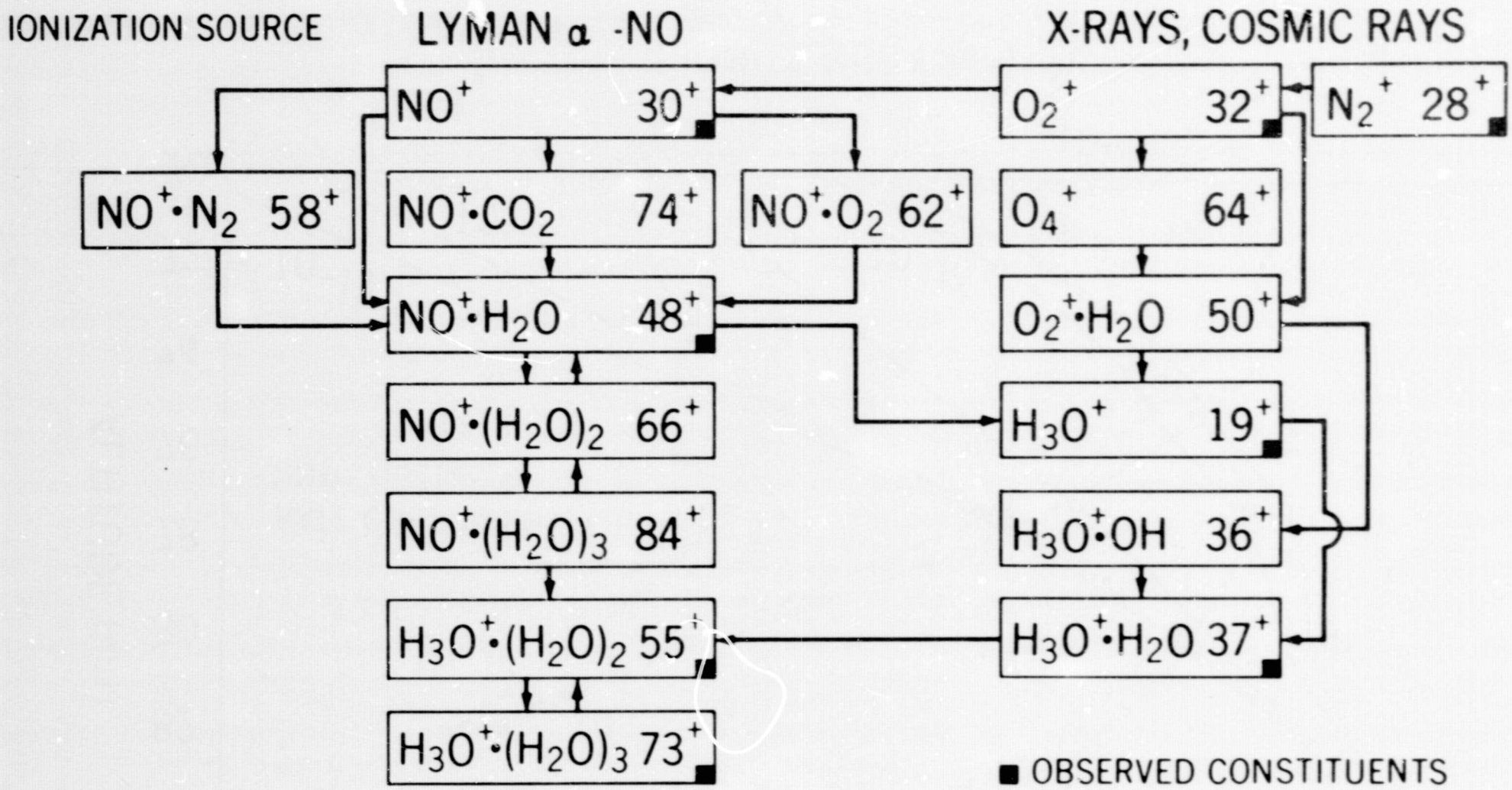
IONIZATION SOURCE
LYMAN α -NO
X-RAYS, COSMIC RAYS
NO+ 30+
O2+ 32+
N2+ 28+
NO+•N2 58+
NO+•CO2 74+
NO+•O2 62+
O4+ 64+
NO+•H2O 48+
O2+•H2O 50+
NO+•(H2O)2 66+
H3O+ 19+
NO+•(H2O)3 84+
H3O+•OH 36+
H3O+•(H2O)2 55+
H3O+•H2O 37+
H3O+•(H2O)3 73+
■ OBSERVED CONSTITUENTS

Figure 7

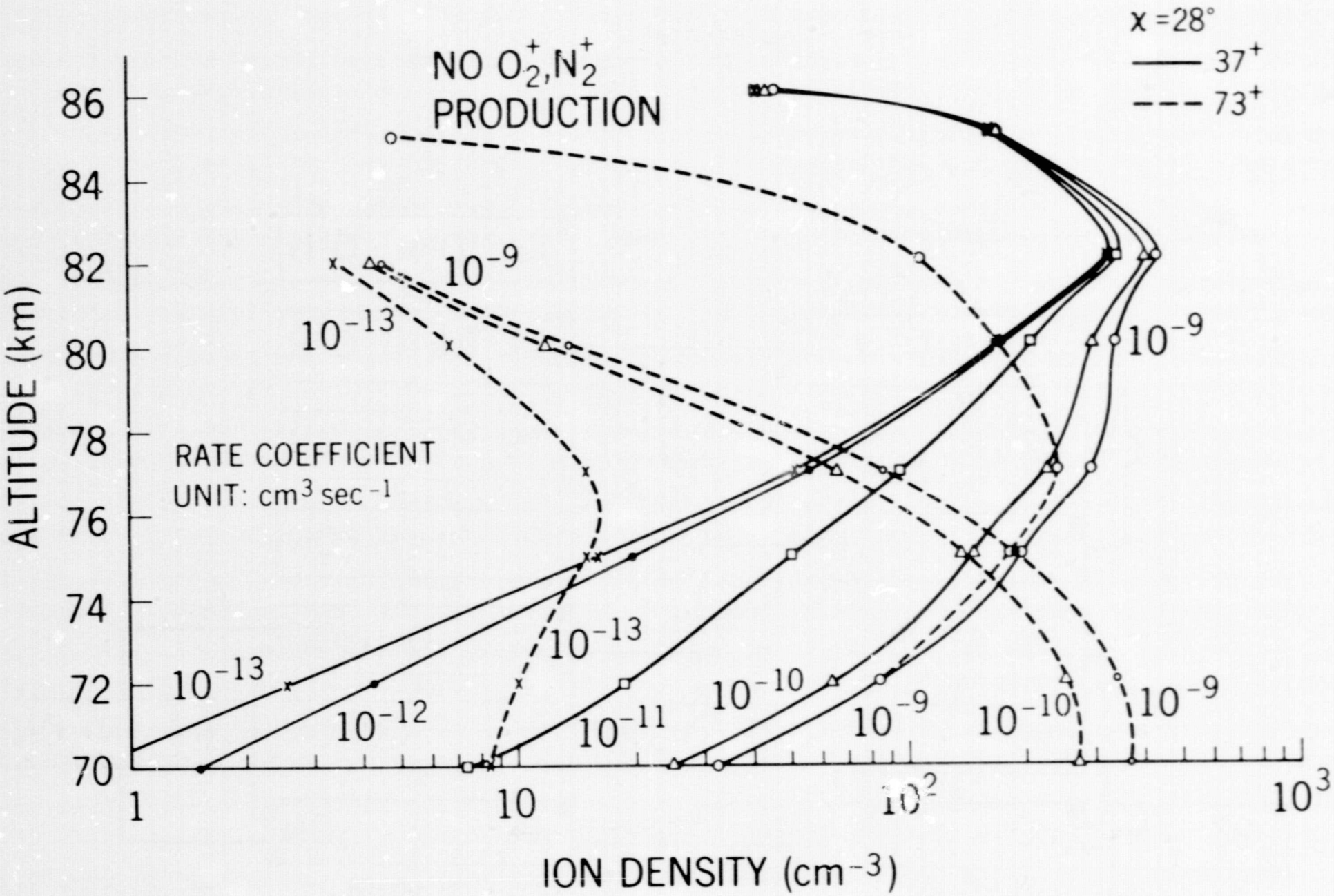
x =28°
37+
73+
NO O2+,N2+
PRODUCTION
10-9
10-13
10-9
RATE COEFFICIENT
UNIT: cm3 sec-1
10-13
10-12
10-13
10-11
10-10
10-9
10-10
10-9
86
84
82
80
78
76
74
72
70
ALTITUDE (km)
1
10
10²
10³
ION DENSITY (cm-3)

Figure 8

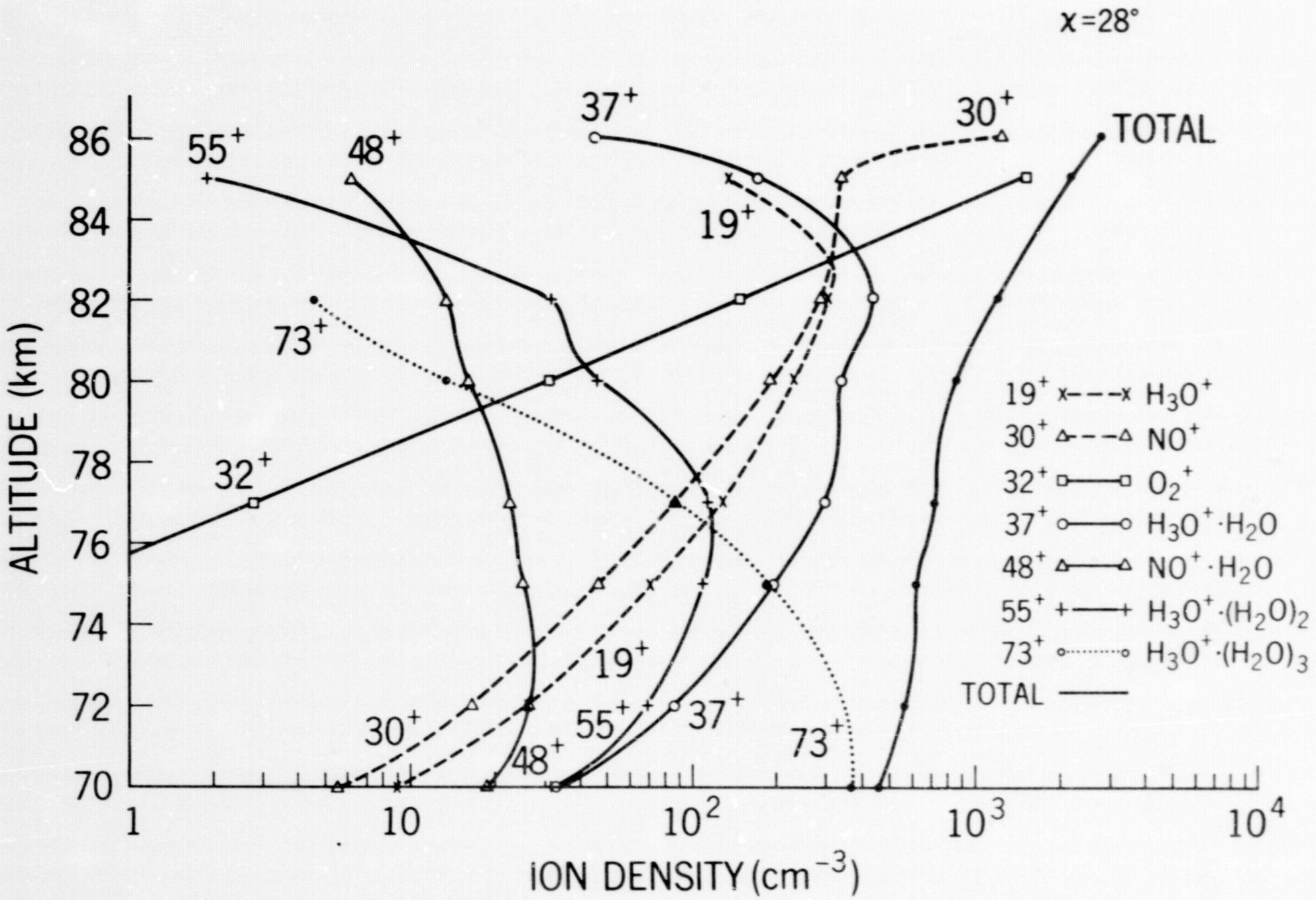
χ=28°
86
84
82
80
78
76
74
72
70
ALTITUDE (km)
1
10
10^2
10^3
10^4
ION DENSITY (cm^{-3})
55^+
48^+
37^+
30^+
TOTAL
19^+
73^+
32^+
19^+
30^+
55^+
37^+
48^+
73^+
19^+ x---x H_3O^+
30^+ △---△ NO^+
32^+ □—□ O_2^+
37^+ ○—○ $H_3O^+ \cdot H_2O$
48^+ △—△ $NO^+ \cdot H_2O$
55^+ +—+ $H_3O^+ \cdot (H_2O)_2$
73^+ ○·····○ $H_3O^+ \cdot (H_2O)_3$
TOTAL ——

Figure 9